

High-mobility transparent conducting Mo-doped In₂O₃ thin films by pulsed laser deposition

C. Warmisingsh, Y. Yoshida, D. W. Readey, C. W. Teplin, J. D. Perkins, P. A. Parilla, L. M. Gedvilas, B. M. Keyes, and D. S. Ginley

Citation: *Journal of Applied Physics* **95**, 3831 (2004); doi: 10.1063/1.1646468

View online: <http://dx.doi.org/10.1063/1.1646468>

View Table of Contents: <http://scitation.aip.org/content/aip/journal/jap/95/7?ver=pdfcov>

Published by the AIP Publishing

Articles you may be interested in

Zn-doped CuAlS₂ transparent p-type conductive thin films deposited by pulsed plasma deposition
J. Vac. Sci. Technol. A **27**, 1316 (2009); 10.1116/1.3244565

High near-infrared transparency and carrier mobility of Mo doped In₂O₃ thin films for optoelectronics applications
J. Appl. Phys. **106**, 063716 (2009); 10.1063/1.3224946

Spray deposited molybdenum doped indium oxide thin films with high near infrared transparency and carrier mobility
Appl. Phys. Lett. **94**, 212101 (2009); 10.1063/1.3142424

Role of Sn doping in In₂O₃ thin films on polymer substrates by pulsed-laser deposition at room temperature
Appl. Phys. Lett. **88**, 151908 (2006); 10.1063/1.2195096

Transparent and semitransparent conducting film deposition by reactive-environment, hollow cathode sputtering
J. Vac. Sci. Technol. A **23**, 1215 (2005); 10.1116/1.1894423

The advertisement features a blue background with a film strip graphic on the left. The text is in white and orange. The main headline reads 'Not all AFMs are created equal' in orange, followed by 'Asylum Research Cypher™ AFMs' in white, and 'There's no other AFM like Cypher' in orange. Below this is the website 'www.AsylumResearch.com/NoOtherAFMLikeIt' in white. In the bottom right corner is the Oxford Instruments logo, which consists of the word 'OXFORD' above 'INSTRUMENTS' inside a square frame, with the tagline 'The Business of Science®' below it.

Not all AFMs are created equal
Asylum Research Cypher™ AFMs
There's no other AFM like Cypher
www.AsylumResearch.com/NoOtherAFMLikeIt
OXFORD
INSTRUMENTS
The Business of Science®

High-mobility transparent conducting Mo-doped In_2O_3 thin films by pulsed laser deposition

C. Warm Singh, Y. Yoshida, and D. W. Readey
Colorado School of Mines, Golden, Colorado 80401

C. W. Teplin, J. D. Perkins,^{a)} P. A. Parilla, L. M. Gedvilas, B. M. Keyes, and D. S. Ginley
National Renewable Energy Laboratory, 1617 Cole Boulevard, Golden, Colorado 80401

(Received 30 October 2003; accepted 16 December 2003)

Highly conductive and transparent Mo-doped indium oxide (IMO) thin films were grown on glass and (100) yttria-stabilized zirconia (YSZ) single-crystal substrates by pulsed laser deposition. The electrical, optical, and structural properties were measured for films grown from 0, 1, 2, and 4 wt % Mo-doped targets. Films grown from the 2 wt % Mo-doped target had the best overall properties. In particular, for biaxially textured 2 wt % Mo IMO films grown on (100) YSZ, the conductivity was $\sim 3000 \text{ S cm}^{-1}$ with a mobility greater than $95 \text{ cm}^2 \text{ V}^{-1} \text{ s}^{-1}$. In the visible, the optical transmittance normalized to the substrate was greater than 90%. © 2004 American Institute of Physics.

[DOI: 10.1063/1.1646468]

Transparent conducting oxides (TCOs) are important in thin-film photovoltaics, smart windows, organic light-emitting diodes, and flat-panel displays.¹ For improved TCOs, the key requirement is to develop high mobility materials to increase electrical conductivity without sacrificing optical transparency.² Recently, molybdenum-doped indium oxide (IMO) thin films prepared by thermal reactive evaporation were reported with a conductivity (σ) of 5900 S cm^{-1} , a mobility (μ) greater than $100 \text{ cm}^2 \text{ V}^{-1} \text{ s}^{-1}$, a carrier concentration (n) of $\sim 3 \times 10^{20} \text{ cm}^{-3}$, and transparency greater than 80%.^{3,4} IMO films with $\sigma=1000 \text{ S cm}^{-1}$ and $\mu=44 \text{ cm}^2 \text{ V}^{-1} \text{ s}^{-1}$ ($n=1.4 \times 10^{20} \text{ cm}^{-3}$) have now also been grown by rf sputtering from a 4 wt % Mo- In_2O_3 target.⁵ For comparison, commercial indium tin oxide (ITO) on glass has $\sigma=5000 \text{ S cm}^{-1}$ with $\mu=47 \text{ cm}^2 \text{ V}^{-1} \text{ s}^{-1}$ ($n=6.6 \times 10^{20} \text{ cm}^{-3}$)⁶ and research grade ITO films grown on yttria-stabilized zirconia (YSZ) by pulsed laser deposition have $\sigma=13\,000 \text{ S cm}^{-1}$ with $\mu=42 \text{ cm}^2 \text{ V}^{-1} \text{ s}^{-1}$ ($n=1.9 \times 10^{21} \text{ cm}^{-3}$).⁷ Routine deposition of TCOs with high mobility would be a significant advance. Accordingly, we are investigating IMO as a high mobility TCO. One clearly important question is: What is the best molybdenum content?

In this study, pulsed laser deposition (PLD) is used to grow IMO thin films from indium oxide targets with various molybdenum concentrations. IMO films grown on (100) YSZ substrates were biaxially textured. The electrical and optical properties of IMO films deposited from the 2 wt % Mo- In_2O_3 target were superior to those deposited from either the 1 or 4 wt % Mo- In_2O_3 targets.

IMO films were grown by PLD from 1 in. diameter pure In_2O_3 and Mo-metal-doped In_2O_3 targets. The targets from Cerac, Inc. were made by sintering a mixture of metallic Mo with In_2O_3 . The approximate target stoichiometries are 1 wt % Mo in In_2O_3 ($\text{In}_{1.97}\text{Mo}_{0.03}\text{O}_{3+\delta}$), 2 wt % Mo

($\text{In}_{1.94}\text{Mo}_{0.06}\text{O}_{3+\delta}$), and 4 wt % Mo ($\text{In}_{1.88}\text{Mo}_{0.12}\text{O}_{3+\delta}$). A KrF excimer laser (248 nm, 300 mJ per pulse, pulse rate of 10 Hz, 45° incident angle, $1 \times 3 \text{ mm}^2$ spot) was used for the target ablation. Films were deposited on both glass (Corning No. 1737) and single-crystal YSZ (100) substrates. All the films were grown in pure O_2 at 2×10^{-3} Torr at a substrate temperature of 500°C .

Cu $K\alpha$ x-ray diffraction (XRD) radiation was used to study the film crystal structure. Film electrical properties were obtained from van der Pauw-style Hall measurements at room temperature on an area of $1 \times 1 \text{ cm}^2$. The optical transmission and reflection from 0.3 to $1.8 \mu\text{m}$ are measured using a fiber-coupled charge coupled device array spectrometer at normal incidence. The IR transmission and reflection from 1.8 to $8 \mu\text{m}$ are measured using a Fourier-transform infrared spectrometer at normal and 30° incidence, respectively. The film thickness was measured with stylus profilometry.

Figure 1(a) shows the $\theta/2\theta$ XRD spectrum for a 4 wt % Mo film on a YSZ substrate. The XRD spectra of a 2 wt % Mo film on YSZ and a blank YSZ substrate are shown in Figs. 1(b) and 1(c), respectively. The peak positions from the JCPDS file for In_2O_3 are shown in the bottom panel.⁸ All the nonsubstrate $\theta/2\theta$ XRD peaks are indexed to In_2O_3 . The four strongest peaks at 17.5° , 35.5° , 54.5° , and 74.9° (+) are indexed to In_2O_3 peaks. The (222) and (444) peaks (*) were also observed in a 4 wt % Mo film. No other compounds were observed in the films on YSZ. The XRD (211) pole figure of the 2 wt % Mo film is shown in the inset. All four spots expected at $\chi=35^\circ$ and eight spots expected at $\chi=65^\circ$ for the (211) pole of In_2O_3 were observed, indicating that the 2 wt % Mo film is (100)-oriented and biaxially textured.

The $\theta/2\theta$ XRD spectra of IMO films on glass deposited from (a) 4 wt % Mo, (b) 2 wt % Mo, and (c) pure In_2O_3 targets are shown in Fig. 2. As the Mo concentration increases, the films become more textured, as can be seen from the increase in the relative intensity of the (222) peaks. All of

^{a)}Electronic mail: john.perkins@nrel.gov

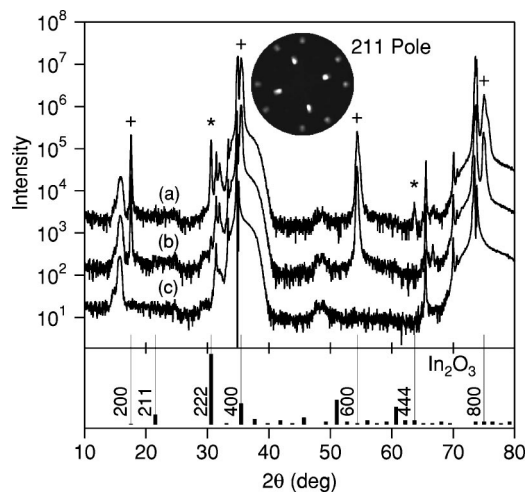


FIG. 1. The $\theta/2\theta$ XRD spectra of (a) 4 wt % Mo, (b) 2 wt % Mo films, and (c) YSZ blank substrate. Note that the intensity in the top panel is shown on a log scale.

the XRD peaks of the film deposited from the 2 wt % Mo target are indexed to In_2O_3 . However, for the film deposited from the 4 wt % Mo target, three additional peaks were observed. Two of these are the In_2O_3 (222) $\text{Cu } K_\beta$ and $W L_\alpha$ peaks as indicated by β and α in the figure. An additional non- In_2O_3 peak is observed at $2\theta=14^\circ$.⁹

The conductivity (σ), mobility (μ), and carrier concentration (n) for the films as determined by Hall measurements are shown in Fig. 3. Closed circles and open triangles represent films on YSZ and films on glass, respectively. Solid lines and dotted lines are drawn through the averages for films on YSZ and glass, respectively. The upper dotted line in panel (c) is the carrier concentration that would arise from 1 e/Mo. All the films have n -type conductivity. The Mo-doped In_2O_3 films have much higher conductivity, mobility, and carrier concentration than the pure In_2O_3 films. The pure In_2O_3 film on YSZ has $n=5.3\times 10^{18} \text{ cm}^{-3}$. Adding 1 wt % Mo dopant ($\text{In}_{1.93}\text{Mo}_{0.03}\text{O}_{3+\delta}$) increased the carrier concentration 25-fold to $1.3\times 10^{20} \text{ cm}^{-3}$. The carrier concentration

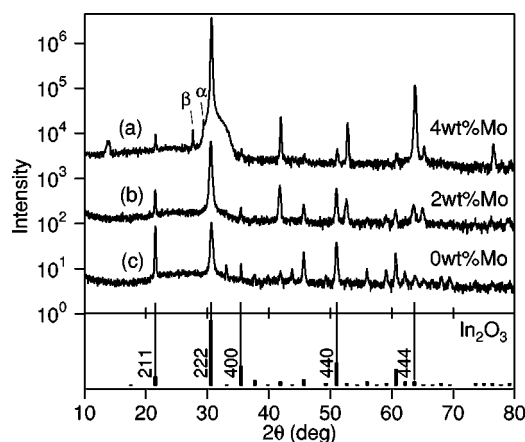


FIG. 2. The $\theta/2\theta$ XRD spectra of (a) 4 wt % Mo, (b) 2 wt % Mo, and (c) pure In_2O_3 films on glass. Note that the intensity in the top panel is shown on a log scale.

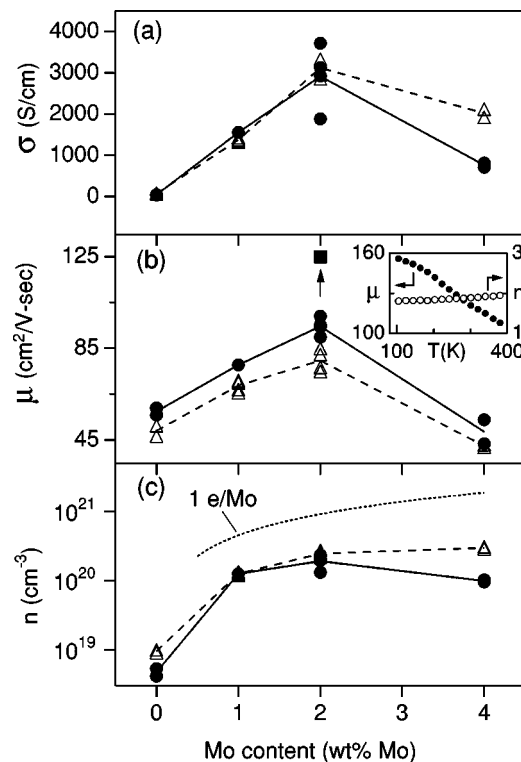


FIG. 3. Electrical properties of pure and Mo-doped In_2O_3 films on YSZ (closed circles) and films on glass (open triangles). In the inset, μ has units of $\text{cm}^2 \text{ V}^{-1} \text{ s}^{-1}$ and n has units of 10^{20} cm^{-3} .

changed only slightly when the Mo concentration increased to 2 wt %.

The electrical properties are best for the films deposited from the 2 wt % Mo target. The 2 wt % Mo films on YSZ have $\sigma=2900 \text{ S cm}^{-1}$ with $n=1.9\times 10^{20} \text{ cm}^{-3}$ and $\mu=95 \text{ cm}^2 \text{ V}^{-1} \text{ s}^{-1}$. When the Mo concentration increased from 2 to 4 wt %, the mobility decreased substantially to less than $50 \text{ cm}^2 \text{ V}^{-1} \text{ s}^{-1}$ (panel b) whereas the carrier concentration remained relatively constant (panel c). The mobility and carrier concentration as a function of temperature for a 2 wt % Mo film on YSZ are shown as an inset to Fig. 3. This film has $\sigma=3800 \text{ S cm}^{-1}$ with $n=1.9\times 10^{20} \text{ cm}^{-3}$ and $\mu=125 \text{ cm}^2 \text{ V}^{-1} \text{ s}^{-1}$ at room temperature.¹⁰ This is the highest mobility measured in this work and is shown in Fig. 3(b) as a solid square highlighted with an arrow. Upon cooling to 105 K, the mobility increased monotonically to $156 \text{ cm}^2 \text{ V}^{-1} \text{ s}^{-1}$ whereas the carrier concentration remained essentially constant indicating that the carrier concentration is not thermally activated over the temperature range measured.

Optical transmission and reflection measurements from all films show typical TCO behavior—transparency in the visible and near-infrared but absorbing in the UV and reflecting in the IR. A typical measurement from a 2 wt % Mo film on glass is shown in Fig. 4, along with fits to the data developed using the Drude model.² In the visible region, the index of refraction was assumed to be 2.0 (far from the plasma frequency)¹¹ and the principle fitting parameter was the film thickness. The resulting thickness was used to model the IR data, where the full Drude model was implemented, as in Ref. 2. Fitting only n and μ with $m^*=0.3$ and $E_{00}=4$

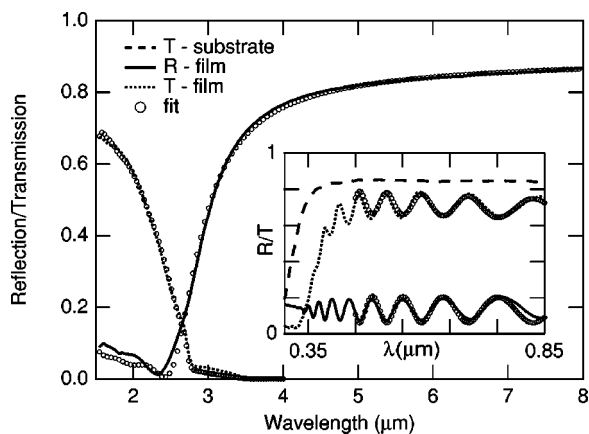


FIG. 4. Optical reflection and transmission of a 2 wt % Mo film.

yields a statistically good result ($\chi^2 < 6$). For the fit in Fig. 4, $\mu = 61.5 \text{ cm}^2 \text{ V}^{-1} \text{ s}^{-1}$ and $n = 1.77 \times 10^{20} \text{ cm}^{-3}$, in reasonable agreement with the electrical results ($\mu = 86.0 \text{ cm}^2 \text{ V}^{-1} \text{ s}^{-1}$, $n = 1.92 \times 10^{20} \text{ cm}^{-3}$), providing confirmation that these are high mobility films.

These PLD-grown IMO films have a conductivity similar to commercial ITO films. But because they have substantially higher mobility, they have a correspondingly lower carrier concentration. The lower carrier concentration extends the transparency (T) further into the infrared and reduces the magnitude of the free-carrier absorption. Modeling shows that, a 1- μm -thick film with $\sigma = 2500 \text{ S cm}^{-1}$ with $\mu = 85 \text{ cm}^2 \text{ V}^{-1} \text{ s}^{-1}$ and $n = 1.8 \times 10^{20} \text{ cm}^{-3}$ will have $T > 70\%$ at $\lambda > 1.5 \mu\text{m}$. However, for the same conductivity but with $\mu = 40 \text{ cm}^2 \text{ V}^{-1} \text{ s}^{-1}$ and $n = 3.9 \times 10^{20} \text{ cm}^{-3}$, $T < 30\%$ of $\lambda = 1.5 \mu\text{m}$. Hence IMO films could have a performance advantage for applications that require higher transparency in the IR range.¹²

IMO films grown by both evaporation^{3,4} and sputtering⁵ also show high mobilities. In their initial work on IMO, Meng *et al.* suggested that perhaps Mo goes into In_2O_3 as Mo^{6+} in place of In^{3+} yielding three electrons per Mo (e/Mo).^{3,4} However, for the films reported here, $0.2 < e/\text{Mo} < 0.3$ for 1 wt % Mo and 2 wt % Mo films. In addition, Yoshida *et al.*⁵ found that $n \leq \sim 3 \times 10^{20} \text{ cm}^{-3}$ for 4 wt % Mo films sputtered in $p_{\text{O}_2} \geq \sim 3 \times 10^{-4} \text{ Torr}$, whereas with lower p_{O_2} , n increases steadily up to $n \approx 1.6 \times 10^{20} \text{ cm}^{-3}$ at $p_{\text{O}_2} \approx 5 \times 10^{-5} \text{ Torr}$. This variation in n with p_{O_2} along with $e/\text{Mo} < 1$ suggest that dopant-metal oxygen-interstitial associates may be the dominant Mo related dopant mechanism similar to the well studied case of Sn substituted In_2O_3 (ITO).¹³⁻¹⁵

In this model, the substitutional Sn dopant in ITO is compensated by interstitial oxygen, $(2\text{Sn}_{\text{In}}^+ \text{O}_i'')^x$ at sufficiently high oxygen pressures.¹⁴ As the oxygen pressure is lowered, the interstitial oxygen is removed, “activating” the Sn dopant via $(2\text{Sn}_{\text{In}}^+ \text{O}_i'')^x \rightleftharpoons 2\text{Sn}_{\text{In}}^+ + 2e' + 1/2\text{O}_2(\text{g})$. The case for IMO is more complicated since there are several possible valence states for Mo in In_2O_3 . For example, Meng *et al.*⁴ suggested that the activated Mo dopant might be $(\text{Mo}_{\text{In}}^{6+} \text{O}_i'')^{\bullet}$ with Mo^{6+} and $e/\text{Mo} = 1$. However, by x-ray

photoelectron spectroscopy, Yoshida *et al.*⁵ found a roughly even mixture of Mo^{6+} and Mo^{4+} in their optimally conducting IMO films but only Mo^{6+} in the low carrier concentration films grown at higher p_{O_2} . This suggests that the activated Mo dopant is not Mo^{6+} ($\text{Mo}_{\text{In}}^{6+}$) but rather Mo^{4+} ($\text{Mo}_{\text{In}}^{4+}$) which might arise from $(2\text{Mo}_{\text{In}}^{6+} 3\text{O}_i'')^x \rightleftharpoons 2\text{Mo}_{\text{In}}^{4+} + 2e' + 3/2\text{O}_2(\text{g})$ which also gives $e/\text{Mo} = 1$. If this is the correct activation reaction, then our finding that $e/\text{Mo} \approx 0.2-0.3$ indicates that not all the Mo atoms are activated, as is known to be the case for Sn in ITO.^{13,14} Note that the In_2O_3 bixbyite structure has two different In sites (25% “b” and 75% “d”) and in the case of ITO, only the b-site Sn is active.¹⁴ If, in these IMO films grown at 500 °C, the Mo randomly occupies the b and d sites and only the b-site Mo can be activated, then the expected average carrier concentration would be $0.25e/\text{Mo}$, very similar to the $0.2-0.3e/\text{Mo}$ found in this work. While there is clearly not yet sufficient data for a definitive determination of the doping mechanism in IMO, we believe that the basic concept of substitutional Mo dopants compensated by interstitial oxygen is both physically reasonable and explains the currently available data.

In summary, Mo-doped In_2O_3 films have been grown by PLD from various Mo-containing targets. It has been shown that biaxial growth of Mo-doped In_2O_3 can be achieved on YSZ (100). The best electrical results were obtained from the $\text{In}_{1.94}\text{Mo}_{0.06}\text{O}_{3+\delta}$ target, where the average mobility is greater than $95 \text{ cm}^2 \text{ V}^{-1} \text{ s}^{-1}$ across a $1 \text{ cm} \times 1 \text{ cm}$ sample. Good correlation is found between the electro-optic properties and the Drude model. Possible point-defect reactions explaining the role of the Mo dopant were proposed.

We thank T. J. Coutts and T. A. Gessert for help and guidance throughout this work. This work was supported by the US Department of Energy Contract No. DE-AC36-99-G010337 through the National Center for Photovoltaics.

¹D. Ginley and C. Bright, MRS Bull. **25**, 15 (2000).

²T. Coutts, D. Young, and X. Li, MRS Bull. **25**, 58 (2000).

³Y. Meng, X. Yang, H. Chen, Y. Jiang, Z. Zhang, and Z. Hua, Thin Solid Films **394**, 219 (2001).

⁴Y. Meng, X. Yang, H. Chen, J. Shen, Y. Jiang, Z. Zhang, and Z. Hua, J. Vac. Sci. Technol. A **20**, 288 (2002).

⁵Y. Yoshida, T. Gessert, C. Perkins, and T. Coutts, J. Vac. Sci. Technol. A **21**, 1092 (2003).

⁶The film was obtained from Applied Film. Hall measurements were done on the BioRad system at NREL.

⁷H. Ohta, M. Orita, M. Hirano, H. Tanji, H. Kawazoe, and H. Hosono, Appl. Phys. Lett. **76**, 2740 (2000).

⁸JCPDS Powder Diffraction File, No. 060416 (1997).

⁹This single peak at 14° has the potential to be indexed to Mo-In-O or Mo-O compounds such as $\text{MoO}_{2.8}$, Mo_4O_{11} , $\text{In}_3\text{Mo}_{11}\text{O}_{17}$, $\text{In}_{11}\text{Mo}_{40}\text{O}_{62}$, or $\text{In}_3\text{Mo}_{11}\text{O}_{17}$.

¹⁰The electrical properties were measured on the area of 50 mm^2 after the film was patterned for four-coefficient measurement.

¹¹R. G. Gordon, MRS Bull. **28**, 52 (2000).

¹²D. Young *et al.*, Proceedings of the 29th IEEE Photovoltaic Specialists Conference, New Orleans, LA, May 24, 2002, p. 608.

¹³J. Hwang, D. Edwards, D. Kammler, and T. Mason, Solid State Ionics **129**, 135 (2000).

¹⁴G. B. Gonzalez, J. B. Cohen, J. Hwang, T. O. Mason, J. P. Hodges, and J. D. Jorgensen, J. Appl. Phys. **89**, 2550 (2001).

¹⁵A. J. Freeman, K. R. Poeppelmeier, T. O. Mason, R. P. H. Chang, and T. J. Marks, MRS Bull. **25**, 45 (2000).